A FAST POINT TO POINT INTERACTION MODEL FOR CHARGED PARTICLE BUNCHES BY MEANS OF NONEQUISPACED FAST FOURIER TRANSFORM (NFFT)

T. Flisgen*, G. Pöplau, U. van Rienen, Rostock University, 18059 Rostock, Germany

Abstract

Demanding applications such as heavy ion fusion, high energy colliders and free electron lasers require the study of beam phenomena like space-charge induced instabilities, emittance growth and halo formation. Numerical simulations for instance with GPT (General Particle Tracer, Pulsar Physics) calculate the mutual Coulomb interactions of the tracked particles [5]. The direct summation of the forces is rather costly and scales with $\mathcal{O}(N^2)$. In this paper we investigate a new approach for the efficient calculation of particle-particle interactions: the fast summation by Nonequispaced Fast Fourier Transform (NFFT) [3, 4], whereas the NFFT is a generalization of the well known Fast Fourier Transformation (FFT). We describe the algorithm and discuss the performance and accuracy of this method for several particle distributions.

INTRODUCTION

The design of particle accelerators requires a sophisticated understanding of the dynamic behaviour of the particle bunch. Therefore several algorithms have been developed to determine the trajectories of the particles in the six-dimensional phase space.

Assuming the energy spread of the charged particles to be small, the space-charge forces may be computed in the bunch's rest frame by superposing the electrostatic field of each particle. The electric field at the position of the j-th particle $\boldsymbol{r}_j \in \mathbb{R}^3$ in the rest frame is given by

$$\boldsymbol{E}(\boldsymbol{r}_j) = \frac{1}{4\pi\varepsilon_0} \sum_{\substack{\ell=1 \\ j\neq\ell}}^{N} q_\ell \frac{\boldsymbol{r}_j - \boldsymbol{r}_\ell}{\|\boldsymbol{r}_j - \boldsymbol{r}_\ell\|^3}, \quad j = 1, \ldots, N, \quad (1)$$

where N denotes the number of particles, q_ℓ the charge of the ℓ-th particle, ε_0 the permittivity of vacuum and $\|\cdot\|$ the Euclidean norm. Since $(N-1)$ interactions have to be taken into account for each of the N particles, the direct evaluation of the sum in Eq. (1) reaches a disadvantageous numerical complexity of $\mathcal{O}(N^2)$. Note that the evaluation of the electric field strength has to be performed in each discrete time step of the tracking to determine the forces acting on the particles.

FAST SUMMATION USING THE NFFT

The presented method calculates the electric fields of the bunch approximately using the Nonequispaced Fast Fourier Transform [3, 4]. The algorithm overcomes the quadratic runtime behaviour of the direct field evaluation and scales with $\mathcal{O}(N \log N)$.

Splitting of Potential Function

To describe the NFFT-based fast field calculation, the potential of a charged particle is separated into a short-range and a long-range effect:

$$\phi(\boldsymbol{r}) = \frac{1}{4\pi\varepsilon_0}\frac{q}{r} = \phi_{sr}(\boldsymbol{r}) + \phi_{lr}(\boldsymbol{r}). \quad (2)$$

Note that $\boldsymbol{r} \in \mathbb{R}^3$ denotes the point in the space, where the potential is evaluated and $r = \|\boldsymbol{r}\| \in \mathbb{R}_{\geq 0}$ the distance between the charged particle (here located at the origin) and the point of field estimation.

We demand the short-range effect $\phi_{sr}(\boldsymbol{r})$ to have compact support, such that $\phi_{sr}(\boldsymbol{r}) = 0 \ \forall \ r \geq \varepsilon_I$ and the long-range effect $\phi_{lr}(\boldsymbol{r})$ to be bounded and $(p-1)$ times differentiable. The variable ε_I denotes the near field radius.

To cope with the singularity at $r = 0$ and to ensure the smoothness of the long-range effect, we regularize the potential at $r = \varepsilon_I$ using an ansatz function (see the dashed, the crossed and the dotted curves in Fig. 1).

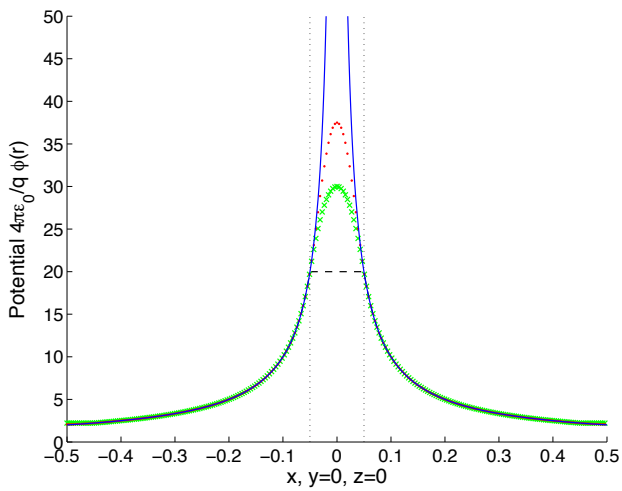

Figure 1: Potential $\phi(\boldsymbol{r})$ (solid) and long-range effect $\phi_{lr}(\boldsymbol{r})$ with $p = 1$ (dashed), $p = 2$ (crossed), $p = 3$ (dotted), where $\varepsilon_I = 1/20$ and $\boldsymbol{r} = (x\ 0\ 0)^T$.

Notice that the potential function is regularized at the boundary $r = l_B = 9/20$ as well to obtain a periodic smooth long-range contribution $\phi_{lr}(\boldsymbol{r})$. The deviation be-

* thomas.flisgen@uni-rostock.de

tween $\phi(\boldsymbol{r})$ and $\phi_{lr}(\boldsymbol{r})$ for $r < \varepsilon_I$ (see Fig. 1) is corrected by the near field potential $\phi_{sr}(\boldsymbol{r})$.

In summary the far field is given by the case differentiation

$$\phi_{lr}(\boldsymbol{r}) = \begin{cases} T_I(\boldsymbol{r}) & \text{if } r < \varepsilon_I, \\ \phi(\boldsymbol{r}) & \text{if } \varepsilon_I \le r \le l_B, \\ T_B(\boldsymbol{r}) & \text{else} \end{cases} \tag{3}$$

and the near field is defined by

$$\phi_{sr}(\boldsymbol{r}) = \begin{cases} \phi(\boldsymbol{r}) - T_I(\boldsymbol{r}) & \text{if } r < \varepsilon_I, \\ 0 & \text{else}, \end{cases} \tag{4}$$

where $T_I(\boldsymbol{r})$ and $T_B(\boldsymbol{r})$ denote the ansatz functions for the inner and outer regularization. It has to be mentioned that the sum of both effects (see Eq. (2)) yields the potential $\phi(\boldsymbol{r})$ only for $r \le l_B$. Thus we have to guarantee by a scaling strategy, which is specified in [1], that the potentials will not be evaluated for particle distances $r > l_B$.

Fourier Construction

Since the long-range potential is $(p-1)$ times continuous differentiable, it can be expressed approximately by the multivariate Fourier sum

$$\phi_{lr}(\boldsymbol{r}) \approx q \sum_{\boldsymbol{k} \in I_n} \hat{b}_{\boldsymbol{k}} \, \mathrm{e}^{2\pi \mathrm{i} \boldsymbol{k} \boldsymbol{r}}, \tag{5}$$

where $\hat{b}_{\boldsymbol{k}} \in \mathbb{C}^{n \times n \times n}$ are the Fourier coefficients of the long-range effect. These coefficients are obtained by equispaced sampling of $\phi_{lr}(\boldsymbol{r})$ and Fast Fourier Transform of the resulting sample values [1, 3, 4]. It is worth to mention that the multi-index $\boldsymbol{k} = (k_x \; k_y \; k_z)$ runs over the finite set

$$I_n := \{-n/2, \ldots, n/2 - 1\}^3, \tag{6}$$

where n^3 is the total number of Fourier coefficients.

Superposition of Field Contributions

Due to the fact that we have to compute potentials of charges located at different positions $\boldsymbol{r}_\ell$ in the bunch, we generalize Eq. (2) by replacing $\boldsymbol{r}$ with $\boldsymbol{r} - \boldsymbol{r}_\ell$. This yields

$$\phi(\boldsymbol{r} - \boldsymbol{r}_\ell) = \frac{1}{4\pi\varepsilon_0} \frac{q_\ell}{\|\boldsymbol{r} - \boldsymbol{r}_\ell\|} \tag{7}$$

$$= \phi_{sr}(\boldsymbol{r} - \boldsymbol{r}_\ell) + \phi_{lr}(\boldsymbol{r} - \boldsymbol{r}_\ell). \tag{8}$$

The equation determines the potential of the ℓ-th particle at the position $\boldsymbol{r}$. To compute the potential at the position of the j-th particle in the bunch, we need to sum up the field contributions of the remaining $(N-1)$ particles:

$$\phi_{bu}(\boldsymbol{r}_j) = \frac{1}{4\pi\varepsilon_0} \sum_{\substack{\ell=1 \\ j \ne \ell}}^{N} \frac{q_j}{\|\boldsymbol{r}_j - \boldsymbol{r}_\ell\|} \tag{9}$$

$$= \sum_{\substack{\ell=1 \\ j \ne \ell}}^{N} \phi_{sr}(\boldsymbol{r}_j - \boldsymbol{r}_\ell) + \sum_{\substack{\ell=1 \\ j \ne \ell}}^{N} \phi_{lr}(\boldsymbol{r}_j - \boldsymbol{r}_\ell). \tag{10}$$

As a result of the compact support of $\phi_{sr}(\boldsymbol{r})$ it has a contribution to the left sum of Eq. (10) only for small distances $\|\boldsymbol{r}_j - \boldsymbol{r}_\ell\| < \varepsilon_I$. Thus we do not need to sum over all ℓ (except $\ell = j$), which would lead to an $\mathcal{O}(N^2)$ runtime behaviour of the algorithm. Instead we need to sum up over the index set

$$I_{\varepsilon_\mathrm{I}}^{\mathrm{NE}}(j) = \{\ell \in \{1, \ldots, N\} : 0 < \|\boldsymbol{r}_j - \boldsymbol{r}_\ell\| < \varepsilon_\mathrm{I}\}, \tag{11}$$

where only the cases $\phi_{sr}(\boldsymbol{r_j} - \boldsymbol{r_\ell}) \ne 0$ are considered. It is worth to mention that a sorting algorithm has to be implemented, which determines the near field particles for all of the N particles.

According to the previous considerations the long-range effect in the right sum of Eq. (10) can be replaced by the Fourier sum Eq. (5):

$$\begin{aligned} \phi_{bu}(\boldsymbol{r}_j) = & \sum_{\ell \in I_{\varepsilon_\mathrm{I}}^{\mathrm{NE}}(j)} \phi_{sr}(\boldsymbol{r}_j - \boldsymbol{r}_\ell) \\ & + \sum_{\substack{\ell=1 \\ j \ne \ell}}^{N} q_\ell \sum_{\boldsymbol{k} \in I_n} \hat{b}_{\boldsymbol{k}} \, \mathrm{e}^{2\pi \mathrm{i} \boldsymbol{k} (\boldsymbol{r}_j - \boldsymbol{r}_\ell)}. \end{aligned} \tag{12}$$

The difference in the exponent of the e-function will be separated and written as a product of two exponential functions. This yields

$$\begin{aligned} \phi_{bu}(\boldsymbol{r}_j) = & \sum_{\ell \in I_{\varepsilon_\mathrm{I}}^{\mathrm{NE}}(j)} \phi_{sr}(\boldsymbol{r}_j - \boldsymbol{r}_\ell) - q_j \sum_{\boldsymbol{k} \in I_n} \hat{b}_{\boldsymbol{k}} \\ & + \sum_{\ell=1}^{N} q_\ell \sum_{\boldsymbol{k} \in I_n} \hat{b}_{\boldsymbol{k}} \, \mathrm{e}^{2\pi \mathrm{i} \boldsymbol{k} \boldsymbol{r}_j} \, \mathrm{e}^{-2\pi \mathrm{i} \boldsymbol{k} \boldsymbol{r}_\ell}. \end{aligned} \tag{13}$$

It is highlighted that the summation $\sum_{\ell=1}^{N} \ldots$ in (13) does not exclude the case $j = \ell$ anymore. For the sake of equality we have to preclude this case manually by subtracting the contribution $q_j \sum_{\boldsymbol{k} \in I_n} \hat{b}_{\boldsymbol{k}}$.

Now we rewrite our formula such that it can be expressed by two multivariate Nonequispaced Fast Fourier Transforms:

$$\begin{aligned} \phi_{bu}(\boldsymbol{r}_j) = & \sum_{\ell \in I_{\varepsilon_\mathrm{I}}^{\mathrm{NE}}(j)} \phi_{sr}(\boldsymbol{r}_j - \boldsymbol{r}_\ell) - q_j \sum_{\boldsymbol{k} \in I_n} \hat{b}_{\boldsymbol{k}} \\ & + \underbrace{\sum_{\boldsymbol{k} \in I_n} \hat{b}_{\boldsymbol{k}} \underbrace{\left(\sum_{\ell=1}^{N} q_\ell \, \mathrm{e}^{-2\pi \mathrm{i} \boldsymbol{k} \boldsymbol{r}_\ell} \right)}_{\mathrm{NFFT^T}} \mathrm{e}^{2\pi \mathrm{i} \boldsymbol{k} \boldsymbol{r}_j}}_{\mathrm{NFFT}}. \end{aligned} \tag{14}$$

The summation in the inner brackets denotes a transposed version of the NFFT. The outer summation denotes a NFFT. These transforms can be calculated very efficiently by using the software library of Kunis and Potts [2].

Determination of Electric Field Strength

Since the electric field strength of the bunch at the position $\boldsymbol{r}_j$ is needed for the tracking procedure, we have to

evaluate the gradient of our potential:

$$\boldsymbol{E}(\boldsymbol{r}_j) = -\nabla\phi_{bu}(\boldsymbol{r}_j). \tag{15}$$

Exemplarily only the x-component $E_x(\boldsymbol{r}_j)$ of the electric field is discussed. Therefore we have to estimate the partial derivation $\frac{\partial}{\partial x_j}$ of the derived potential given in Eq. (14):

$$E_x(\boldsymbol{r}_j) = -\sum_{\ell\in I_{\varepsilon_I}^{\mathrm{NE}}(j)} \frac{\partial}{\partial x_j}\phi_{sr}(\boldsymbol{r}_j - \boldsymbol{r}_\ell)$$
$$-\underbrace{\sum_{\boldsymbol{k}\in I_n} 2\pi\mathrm{i}\, k_x\, \hat{b}_{\boldsymbol{k}} \underbrace{\left(\sum_{\ell=1}^{N} q_\ell\, \mathrm{e}^{-2\pi\mathrm{i}\boldsymbol{k}\boldsymbol{r}_\ell}\right)}_{\mathrm{NFFT^T}} \mathrm{e}^{2\pi\mathrm{i}\boldsymbol{k}\boldsymbol{r}_j}}_{\mathrm{NFFT}}. \tag{16}$$

Again the summation in the inner brackets denotes a transposed NFFT. This is followed by n^3 multiplications with $2\pi\mathrm{i}\, k_x\, \hat{b}_{\boldsymbol{k}}$. Finally the outer summation is computed by a NFFT. The transforms are performed by the library [2].

To ensure an advantageous runtime behaviour of the algorithm, we define the near field radius depending on the number of particles:

$$\varepsilon_I = \frac{p}{2\sqrt[3]{N}}. \tag{17}$$

The order of smoothness is set to $p = 3$ and the total number of Fourier coefficients to $n \approx \sqrt[3]{N}$.

BENCHMARKING THE ALGORITHM

The presented algorithm has been implemented in C and tested on an Intel(R)-Xeon(TM)-3 GHz machine with 4 GB RAM using Windows Server 2003.

Error Definitions

Beside the runtime behaviour of the algorithm which we compare with the runtime of the direct summation Eq. (1), we discuss the accuracy of the method. Therefore we define the relative error in the electric field strength by

$$f_j = \frac{\|\boldsymbol{E}_{nfft}(\boldsymbol{r}_j)\| - \|\boldsymbol{E}(\boldsymbol{r}_j)\|}{\|\boldsymbol{E}(\boldsymbol{r}_j)\|}, \quad j = 1,\ldots,N, \tag{18}$$

where $\|\boldsymbol{E}_{nfft}(\boldsymbol{r}_j)\|$ is the absolute value of the strength computed by Eq. (16). The field strength $\|\boldsymbol{E}(\boldsymbol{r}_j)\|$ is determined by the direct summation Eq. (1). Additionally we consider the maximum of the relative error given by

$$f_{max} = \max_{j=1}^{N} |f_j|. \tag{19}$$

Spherical Distribution

Initially a spherical particle distribution is considered. The radius of the sphere amounts to $R = 2.2\,\mathrm{mm}$. Fig. 2 shows the runtime for the direct summation (see Eq. (1)) and the NFFT-based summation (see Eq. (16).

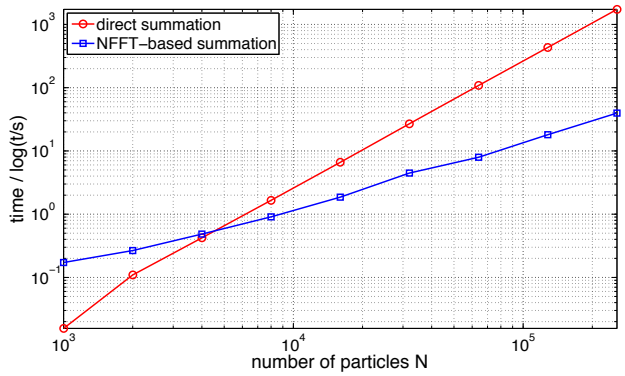

Figure 2: Runtime comparison for a spherical particle distribution using a logarithmic scaling of axes.

Note that logarithmic scales are used for both axes. The ⊙-curve documents the $\mathcal{O}(N^2)$ runtime behaviour of the direct field evaluation, whereas the ⊡-curve shows the beneficial $\mathcal{O}(N \log N)$ performance of the NFFT-approach. Moreover Fig. 2 demonstrates that the approach becomes faster than the direct summation for $N > 4500$ particles. For less particles the proposed algorithm is slower due to its overhead e.g. the computation of the Fourier coefficients in Eq. (5).

Fig. 3 plots the error in the field strength in dependence on the particle location $\boldsymbol{r}_j$. The error is encoded by the colour and the size of the particle. It is obvious that the field values in the center of the distribution are afflicted with larger relative errors. The maximal relative error in the electric field strength is $f_{max} \approx 0.0188$.

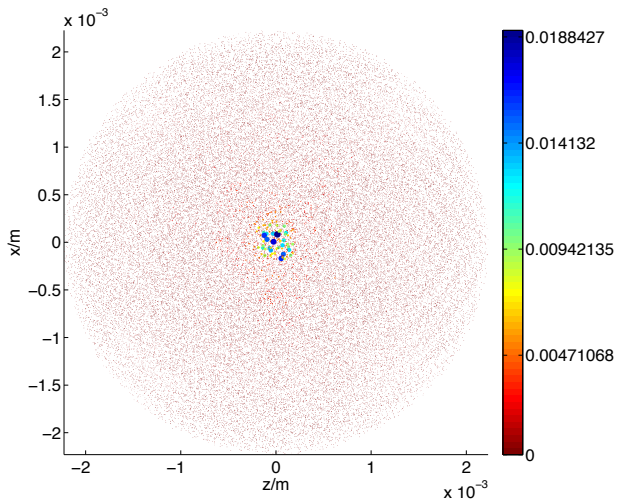

Figure 3: Locations of the relative errors $|f_j|$ for the spherical distribution with $N = 64000$ particles encoded by the colour and the size of the particles.

It is mentionable that larger relative errors in the center of the distribution result in small absolute errors, since the field strengths are small in the center of the charged bunch.

Cylindrical Distribution

Secondly a cylindrical distribution is taken into account. It has a length of $L = 3.5\,\mathrm{mm}$ and a radius of $R = 2\,\mathrm{mm}$. For this case the runtime behaviour of the algorithm is very similar to Fig. 2 [1].

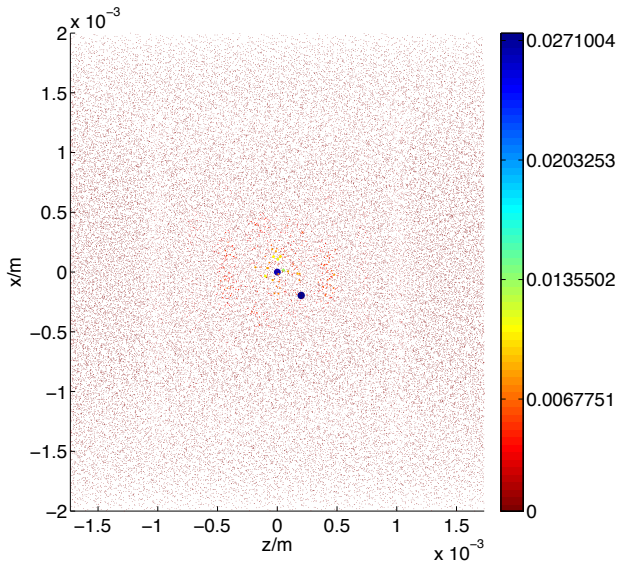

Figure 4: Locations of the relative errors $|f_j|$ for the cylindrical bunch with $N = 64000$ particles encoded by the colour and the size of the particles.

Fig. 4 reflects the error $|f_j|$ for the cylindrical particle distribution. The maximal error is $f_{max} \approx 0.027$. Note that the "hard edges" of the cylinder are difficult to treat numerically (especially with mesh-based strategies for field evaluation) and analytically. Despite this fact the largest relative error is again in the center of the distribution.

Sandwich Distribution

Finally a sandwich distribution is examined. It is constructed of ten flat ellipsoidal bunches arranged in series. The semi-axes of the bunches are $R_x = R_y = 1\,\mathrm{mm}$ in the transversal direction and $R_z = 0.025\,\mathrm{mm}$ in the longitudinal direction. The distance between the bunches is $\Delta d = 0.111\,\mathrm{mm}$. The runtime behaviour of the algorithm for the sandwich distribution is analog to Fig. 2, but in contrast to that plot the point of intersection is now at $N \approx 6000$ [1].

Fig. 5 shows the geometry and illustrates the error $|f_j|$ in the absolute electric field strength for each particle. The maximal relative error is $f_{max} \approx 0.032$. It is remarkable that larger errors are not located on the boundary of the flat ellipsoidal bunches, but again in the center of the whole distribution.

CONCLUSIONS

In this paper a method for the efficient calculation of electric fields inside a bunch of charged particles is constructed. The presented algorithm overcomes the quadratic runtime of the direct summation and scales for the proposed examples with $\mathcal{O}(N \log N)$. Although it is still slower compared to mesh-based methods, it has the advantage that it copes very well with "hard edges" and discontinuities in the charge density ρ.

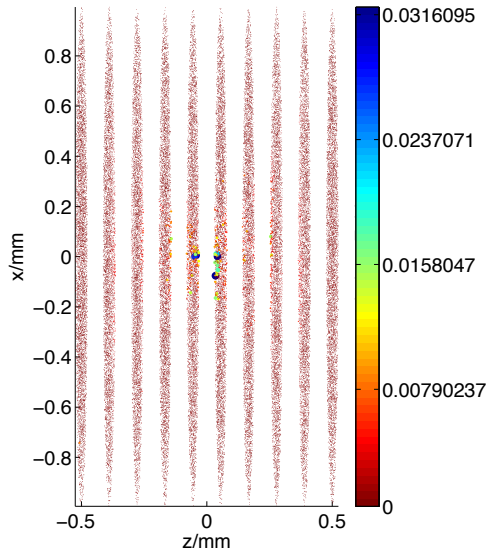

Figure 5: Locations of the relative errors $|f_j|$ for the sandwich bunch with $N = 64000$ particles encoded by the colour and the size of the particles.

It is spotlighted that the time evolution of the bunch's shape is mainly determined by the forces on the particles located at the boundary of the distribution. Therefore especially the field values at the edges have to be computed with small errors. Hence larger relative errors in the center of the distribution pose no crucial problem for the tracking.

REFERENCES

[1] T. Flisgen. *Implementation of a Fast Point to Point Interaction Model for Charged Particle Bunches by means of NFFT*. Master thesis, Rostock University, 2009.

[2] S. Kunis and D. Potts. NFFT, Softwarepackage, C subroutine library. `http://www-user.tu-chemnitz.de/~potts/nfft/`, 2002 – 2004.

[3] G. Pöplau, D. Potts, and U. van Rienen. Calculation of 3D space-charge fields of bunches of charged particles by fast summation. In A. Anile, G. Alì, and G. Mascaly, editors, *Scientific Computing in Electrical Engineering*, number 9 in Mathematics in Industry, pages 241–246, Berlin, 2006. Springer-Verlag.

[4] D. Potts and G. Steidl. Fast summation at nonequispaced knots by NFFTs. SIAM *J. Sci. Comput.*, 24:2013 – 2037, 2003.

[5] S. van der Geer and M. de Loos. *The General Particle Tracer Code. Design, implementation and application*. PhD thesis, TU Eindhoven, 2001.